

## PHOTOINJECTOR WITH BOOSTER SECTION FOR CTF2

*R. Bossart and M. Dehler*

### 1. INTRODUCTION

An extra klystron MDK 29 with an output power of 35 MW will become available for CTF in 1997. With this additional klystron it will be possible to feed the rf sections of the probe beam separately from the rf gun of the drive beam fed by klystron MDK 98, and to run the rf gun of the drive beam at a slightly higher frequency for better compensation of the heavy beam loading. The additional rf power allows also the doubling of the beam energy of the photoinjector by the existing booster section for better injection into the high charge sections HCS and avoids beam blow-up at high intensity and low beam energy at the entrance of the first HCS section [1]. The layout of the upgraded photoinjector with two rf sections and an intermediate focusing solenoid is shown in Figs. 1 and 2.

### 2. COMPENSATION OF BEAM LOADING BY PHASE VARIATION OF RF GUN

For nominal operation, the gun of the drive beam for CTF 2 produces a bunch train of  $48 \times 13.5 \text{ nC} = 650 \text{ nC}$  total charge. Because of the high beam intensity produced, the beam energy at the exit of gun 4 decays linearly from 7.0 MeV for the first bunch to 5.7 MeV for the last bunch. The energy decay along the bunch train causes a lower beam velocity in the gun and in the drift space after the gun. The flight time of the bunches from the photocathode to the gun exit increases during the bunch train by 6.7 ps, and by 2.7 ps in the drift space of length 0.63 m (see Figs. 6-7 of Ref. [5]). The increase of the flight time by 9.4 ps along the bunch train of 15.7 ns duration causes a frequency shift  $\Delta f/f = 0.6 \times 10^{-3}$  of the bunch repetition frequency in the 30 GHz power transfer structures. As the 30 GHz frequency component of the drive beam is reduced by  $0.6 \times 10^{-3}$ , the acceleration of the probe beam by the structures CAS is reduced to 93% of the nominal energy gain. The repetition frequency of the bunch train reduced by -1.8 MHz causes large phase errors of  $10^\circ$  to the beam loading correction scheme with the HCS sections designed for  $2\,998.5 \pm 7.8 \text{ MHz}$ . The frequency difference between the beam and the HCS sections changes with the beam intensity and amounts to +9.6 MHz and -6.0 MHz for 650 nC total beam charge instead of  $\pm 7.8 \text{ MHz}$ .

In order to stabilize the flight time of the bunch train of 650 nC, the radiofrequency of gun 4 must be increased by 3.5 MHz to 3 002.1 MHz. Thereby, the rf phase between the gun and the laser pulses with a repetition frequency of 2 998.55 MHz is gradually shifted from  $20^\circ$  for the first bunch to  $40^\circ$  for the last bunch, so that the flight time of the beam in the gun stays nearly constant for all bunches according to beam simulations with MAFIA (Fig. 3).

Because of the beam loading by 650 nC, the rf field in the gun decays from 100 MV/m peak for the first bunch to 80 MV/m peak for the last bunch.

For accurate stabilisation of the beam flight time, the frequency offset of the gun must be adjusted proportionally to the total charge of the drive beam. The rf frequency can be offset by a programmable phase shifter in the low power rf drive of the klystron MDK 98. Unfortunately, the resonant frequency of the gun can be increased only by 2 MHz by means of the mobile tuners, and a new tuner design would be required for gun 4.

In gun 5 the stored energy of the first cell is three times larger than for gun 4, and the phase slip of the beam due to beam loading is three times smaller. It is expected for gun 5 that a frequency increase of about 1.5 MHz is sufficient to stabilize the flight time of a bunch train of  $48 \times 13.5$  nC. MAFIA simulations for gun 5 will be carried out in 1997 to confirm the exact amount of phase shift required for constant flight time of the bunch train.

A second method to compensate the increasing flight time of the bunch train in the gun is offered by the laser pulse train generator. However, the laser pulse interval of the train cannot be changed easily during operation.

The pulse train generator of the laser splits a single laser pulse into a pulse train of 48 equidistant bunches with a pulse interval corresponding exactly to the wavelength  $\lambda$  of the accelerating frequency of the gun. If the distance between laser pulses is reduced from  $\lambda = 100.00$  mm to 99.92 mm, the last laser pulse hits the photocathode -3.8 mm in advance of the synchronous bunch interval  $47\lambda$ . The reduced laser pulse interval results in a strongly non-linear correction of the flight time towards the end of the bunch train (see Fig. 3).

In a third method for better linear correction, the pulse interval of the laser pulse train generator is adjusted for  $L = 99.96$  mm, and the rf phase of the accelerating field in the gun is increased between the first and last bunch. By employing both methods together, the variable rf phase shifting and the fixed laser pulse interval of  $0.9996 \lambda$ , the frequency offset required for gun 4 is reduced to +1.3 MHz for a bunch train of  $48 \times 13.5$  nC.

For correct operation of the laser pulse train with or without correction for the increasing beam flight time, the optical beam splitters, mirrors and optical combiners of the laser pulse train generator must be aligned with a precision of better than 0.01 mm, otherwise too large phase errors are accumulated in the optical path of the laser pulse train generator. The mechanical stability and accuracy of the laser pulse train generator is crucial for the correct phasing of the drive beam for the HCS beam loading compensation scheme of CTF2 and for acceleration of the probe beam at 30 GHz.

### **3. IMPROVEMENT OF BEAM STABILITY BY BOOSTER SECTION**

The main motivations for installing a booster section at the exit of the gun are the good results of the old rf booster with four cells accelerating a bunch train of 48 bunches with 450 nC total charge to 10 MeV in 1994 [2,3]. Since there was not enough rf power available from the klystron MDK 98 in the first layout of CTF2 for 1996, the booster section has not been installed for the drive beam. However, the booster section would be very useful for matching the large beam divergence of the rf gun to the high charge section HCS. The new

photoinjector comprising an rf gun and a booster section would provide a higher beam energy of 17 MeV and a smaller beam radius reducing the transverse beam break-up forces at injection into the travelling wave section HCS. The booster section would prevent a large emittance blow-up at low energy in a relatively long drift space with two solenoid magnets. The classical design of photoinjectors provides a beam energy of 20 MeV, because the emittance blow-up in the drift space after the photoinjector is proportional to  $1/\gamma^3$  [4], where  $\gamma$  is the relativistic factor.

In 1997, about 35 MW of 3 GHz power will become available from klystron MDK 29 which has served so far as spare klystron for the LIL linac. The existing booster section used until 1995 requires an rf power of 15 MW for an electric field strength of 100 MV/m accelerating the first bunch of 7.0 MeV ( $\gamma_1 = 13.9$ ) from the gun to 17.0 MeV ( $\gamma_2 = 33.3$ ) at the booster exit. The transverse space-charge forces after the booster section of the drive beam will be reduced by a factor of  $(\gamma_1/\gamma_2)^2 = 0.17$  and the emittance blow-up in the drift space in front of the HCS section by a factor of  $(\gamma_1/\gamma_2)^3 = 0.07$  as compared to the layout without the booster section.

The aperture of the booster section for the beam is limited by the iris diameter of 30 mm, which is nearly equal to the iris diameter of 30.5 mm for the HCS sections. For the same iris diameter and a similar cell geometry, the normalised shunt impedance  $R'/Q$  of the booster and HCS sections are equal for the accelerating mode. The beam loading parameter of the old four cell booster is  $k_0 = \pi f R/Q = 2\,200$  V/nC [3], and the energy decay along the bunch train of total charge  $q = 48 \times 13.5$  nC amounts to  $\Delta U = 2k_0 q e = 2.9$  MeV. The booster section has an excellent transient beam loading behaviour. There is no extra beam loading by the parasitic monopole modes since their shunt impedance is zero [3].

At the exit of gun 4, a bunch train of 650 nC causes an energy decay of 1.3 MeV [5]. The total energy decay of the gun and booster sections is 4.2 MeV. For a field strength of 100 MV/m in the gun and in the booster section, the beam energy of the first bunch amounts to 17.0 MeV. The relative beam loading compared to the energy gain is 24% for the gun and booster section together. The transient beam loading of the booster section is smaller than for the HCS sections because of the smaller bandwidth of the booster.

The gun 4 requires an rf power of 17 MW during 2.8  $\mu$ s to build up an electric rf field of 100 MV/m peak, the booster section necessitates another 15 MW for the same field strength so that the total rf power amounts to 32 MW which can be supplied either from MDK 29 or from MDK 98 already equipped with a 45 MW klystron.

An important advantage of the rf booster is the short drift length of 175 mm between the gun and booster section which is occupied by a compact solenoid magnet. As the beam energy at the exit of the gun decreases from 7.0 MeV to 5.7 MeV during the bunch train of 650 nC, the flight time of the bunches gradually increases by 6.7 ps in gun 4, but only by 1.2 ps between the gun and the exit of the booster. Along the following drift length of 0.5 m between the rf booster and the HCS section, the flight time increases merely by 0.1 ps compared to 2.7 ps for the actual layout with two solenoid magnets after the gun.

The total flight time increase of 8.0 ps between the first and last bunch can be reduced to 1 ps by a frequency increase of about 1.3 MHz for gun and booster section and for the laser pulse train generator. The resonance frequency of the two standing wave sections -gun and booster- can be manually adjusted for the expected beam loading by the mechanical piston tuners of each cell.

#### 4. RADIAL BEAM SIZE IN THE RF BOOSTER SECTION

At the exit of the gun the beam has gathered a transverse momentum from the radial space-charge forces and from the transverse Lorenz forces of the rf field in the gun. Both the radial space-charge force and the radial Lorenz force are to first order linear forces proportional to the distance of the electrons from the beam axis and from the centre axis of the gun. At low beam intensity, the electrons at the gun exit emerge under an angle  $\vartheta$  proportional to their radial position  $r$  from the gun axis according to Kim [6]:

$$\vartheta = r \frac{e E_z \sin \varphi}{2\gamma m_0 c^2} = \frac{r}{d_1}$$

- $\vartheta$  : beam divergence,
- $E_z$  : maximum accelerating electric field strength in the first half-cell,
- $\varphi$  : phase angle of  $E_z$  when the beam leaves the gun,  $E_z \sin \varphi \cong 76$  MV/m,
- $\gamma m_0 c^2$  : energy of electrons at gun exit,  $\gamma = 13.7$ ,
- $d_1$  : drift length for doubling the beam radius after the gun.

The formula of Kim is a good approximation for a gun with a first cell of length  $\lambda/4$ . In gun 4, the beam divergence has been reduced on purpose by elongating the first half-cell from 25 mm to 33 mm and by a conical backplate around the photocathode which induces a supplementary radial rf field counteracting the space-charge forces at the photocathode. In this way a smaller beam divergence has been obtained for gun 4 with  $d_1 = 240$  mm [5].

For a single bunch of 13.5 nC, the beam characteristics can be interpolated from Table 4 of Ref. [5]. Thereby, the radius of the beam on the photocathode can be reduced to

$$r = 6 \text{ mm} \sqrt{13.5 \text{ nC} / 21 \text{ nC}} = 4.8 \text{ mm}$$

so that the space-charge density is the same as for a bunch of 21 nC and 6 mm radius used in Ref. [5].

The emittance is assumed to be proportional to the bunch charge according to the scaling law of Kim [6]. For the beam energy, energy spread and bunch length at 80 MV/m, an interpolation of second order between 100, 85 and 70 MV/m has been used. In the transverse phase space, the bunch radius and beam divergence have been reduced by a factor 0.8 for constant charge density.

According to Table 1 for a bunch train of  $48 \times 13.5$  nC at the exit of the first solenoid magnet, the first bunch has a maximum beam radius of 8.6 mm and the last bunch 9.1 mm. The beam divergence of the first bunch is 8.3 mrad pk and about zero for the last bunch at the exit of the solenoid.

Table 1

Expected beam characteristics for a single bunch of 13.5 nC charge.

Field strength of gun  $E_z = 100 \dots 80$  MV/m, laser phase =  $30^\circ$ , laser spot radius  $r = 4.8$  mm, laser pulse duration = 8 ps fwhm, magnetic field strength of solenoid = 0.343 T.

	Exit of gun 4	Exit of solenoid
Field strength, $E_z$ [MV/m]	100	80
Emittance, $\epsilon_m$ [mm mrad]	48	50
Beam energy, $\gamma$	13.9	11.4
Energy spread, $\Delta\gamma/\gamma$ [%]	0.66	1.44
Bunch length, $\sigma_z$ [mm]	1.05	1.21
Bunch radius, $\sigma_r$ [mm]	4.6	5.2
Max. bunch radius, $r$ [mm]	6.5	7.4
Divergence, $\vartheta_{rms}$ [mrad]	17	21

If the old rf booster is installed behind the solenoid magnet as in 1995 [3], the beam enters without loss into the booster section with a clearance of about 6 mm between the maximum beam radius and the iris radius of 15 mm.

During acceleration in the booster section, the radial rf forces and the increasing mass of the electrons modify the beam divergence. The envelope of the beam follows an oscillatory trajectory shown in Figs. 4 and 5.

At the entrance of the booster section, the radius of the first bunch has slightly increased to 9.8 mm because of the beam divergence. The last bunch entering the booster section as a perfectly paraxial beam leaves the booster with a smaller radius of 8.5 mm because of the rf focusing in the booster section. At the exit, the transverse beam momentum is re-established and is equal to the momentum at the entrance of the booster, except for the space-charge forces which have been taken into account by the differential equation of the beam envelope in the rf booster.

The radial space-charge force is strongest in the transverse symmetry plane containing the bunch centre. For an ultra-relativistic bunch of half length  $\sigma_z$  and maximum radius  $a$ ,  $\gamma\sigma_z \gg a$ , the maximum space-charge force at radius  $r$  amounts to:

$$F_{sc}(z) = \frac{eQr}{2\pi\epsilon_0 a^2(z) 2\sigma_z \gamma^2(z)}$$

For an electron accelerated parallel to the centre axis  $z$  of the booster section, the transverse rf force at radius  $r$  from the axis amounts to [7]:

$$F_{rf}(z) = \frac{1}{2} eE_z k r \cos(2kz + \varphi_0), \quad k = 2\pi / \lambda,$$

where  $\lambda$  is the rf wavelength and  $z$  is the distance from the entrance of the booster section,  $\varphi_0$  is  $90^\circ$  for a particle riding on the crest of the rf wave.

The growth  $\Delta p$  of the transverse beam momentum imparted by the space-charge forces during the linear acceleration of an ultra-relativistic beam of velocity  $v = \beta c \equiv c$  in a section of length  $L$  is given by

$$\Delta p = \int_0^L F_{sc} \frac{dz}{c\beta} \equiv \frac{eQLr}{4\pi\epsilon_0 a^2 \sigma_z c \gamma_2 \gamma_3},$$

where  $\gamma_2$  and  $\gamma_3$  are the relativistic factors at the entrance and at the exit of the accelerating section.

The growth  $\Delta p$  of the transverse momentum in the booster section for  $r = a$  amounts to:

$$\Delta p = \begin{cases} 5.8 \text{ keV} / c, & \text{first bunch: } a = 8.6 \text{ mm}, \sigma_z = 1.06 \text{ mm}, \gamma_2 = 13.8, \gamma_3 = 33.4 \\ 7.6 \text{ keV} / c, & \text{last bunch: } a = 9.1 \text{ mm}, \sigma_z = 1.23 \text{ mm}, \gamma_2 = 11.3, \gamma_3 = 25.2 \end{cases}$$

The space-charge forces increase the maximum beam divergence  $\vartheta_3$  at the booster exit by  $\Delta\vartheta_3 = \Delta p / \gamma_3 m_0 c = 0.6$  mrad pk. At the booster exit the beam divergence is smaller by a factor  $\gamma_2 / \gamma_3$  than at the exit of the solenoid.

As the beam enters the booster section, there is a strong rf focusing force which reduces the radial beam size. Because of the beam loading of the booster section, the radial rf focusing force decreases linearly during the bunch train to the same proportion as the beam energy decreases. Therefore, the focal length of the rf focusing of the booster section remains nearly constant and decreases only by 10% compensating for the overfocusing of the solenoid magnet between gun and booster.

The focusing technique by a second solenoid magnet instead of the rf booster is very sensitive to the beam energy, and the focal length of the solenoids varies as  $f \sim \gamma^2$ . Convergent beams at low energy undergo strong space-charge forces as the beam radius shrinks to below 3 mm. Overfocusing of the last bunches in the train blows up strongly the bunch train emittance and enhances the risk of beam break-up further down in the beam line.

Thanks to the additional beam energy gained in the booster section, the beam is much more stable against space-charge forces at high beam intensity and against rf beam break-up forces caused by the input couplers of the HCS sections.

## 5. CONCLUSIONS

The increase of the flight time of the bunch train due to the beam loading of the rf gun causes large phase and frequency errors to the beam loading correction scheme of the two HCS sections. It is proposed to stabilize the flight time of the bunch train through the gun and the drift space in front of the HCS sections within  $\pm 1$  ps by installing the existing booster section after the gun and by a frequency shift of the laser pulse train and of the photoinjector by +1.3 MHz, proportionally to the total beam charge of 650 nC. The relative beam loading

of the photoinjector comprising gun 4 and the old booster section amounts to 24% for a 650 nC beam charge. By proper adjustment of the frequency of the klystron and of the rf phase between the gun and the booster section, the effects of the beam loading in the photoinjector can be corrected.

## 6. ACKNOWLEDGEMENTS

One of the authors (RB) would like to thank A. Krusche for his help with MATHCAD.

## 7. REFERENCES

- [1] J. Gao and G. Biennu, *Design of the Accelerating Section for CTF 2*, CLIC Note 268.
- [2] H. Braun et al., *CTF Developments and Results*, Proc. 1995 Particle Accelerator Conf., Dallas, May 1995.
- [3] R. Bossart, J.C. Godot, S. Lütgert, and A. Riche, *Modular Electron Gun Consisting of Two RF Sections and an Intermediate Focusing Solenoid*, NIM A340, 1994, p. 157.
- [4] B.E. Carlsten and R.L. Sheffield, *Photoelectric Injector Design Considerations*, Proc. Linac Conf., Williamsburg, 1988, p. 365.
- [5] R. Bossart, H. Braun, M. Dehler, J.C. Godot, *A 3 GHz Photoelectron Gun for High Beam Intensity*, PS/RF Note 95-25, 1995.
- [6] K.J. Kim, *RF and Space-Charge Effects in Laser-Driven RF Electron Guns*, NIM A275, 1989, p. 201.
- [7] L. Serafini, *Particle Motion in RF Photoinjectors*, Particle Accelerators, 1995, Vol. 49, p. 253.

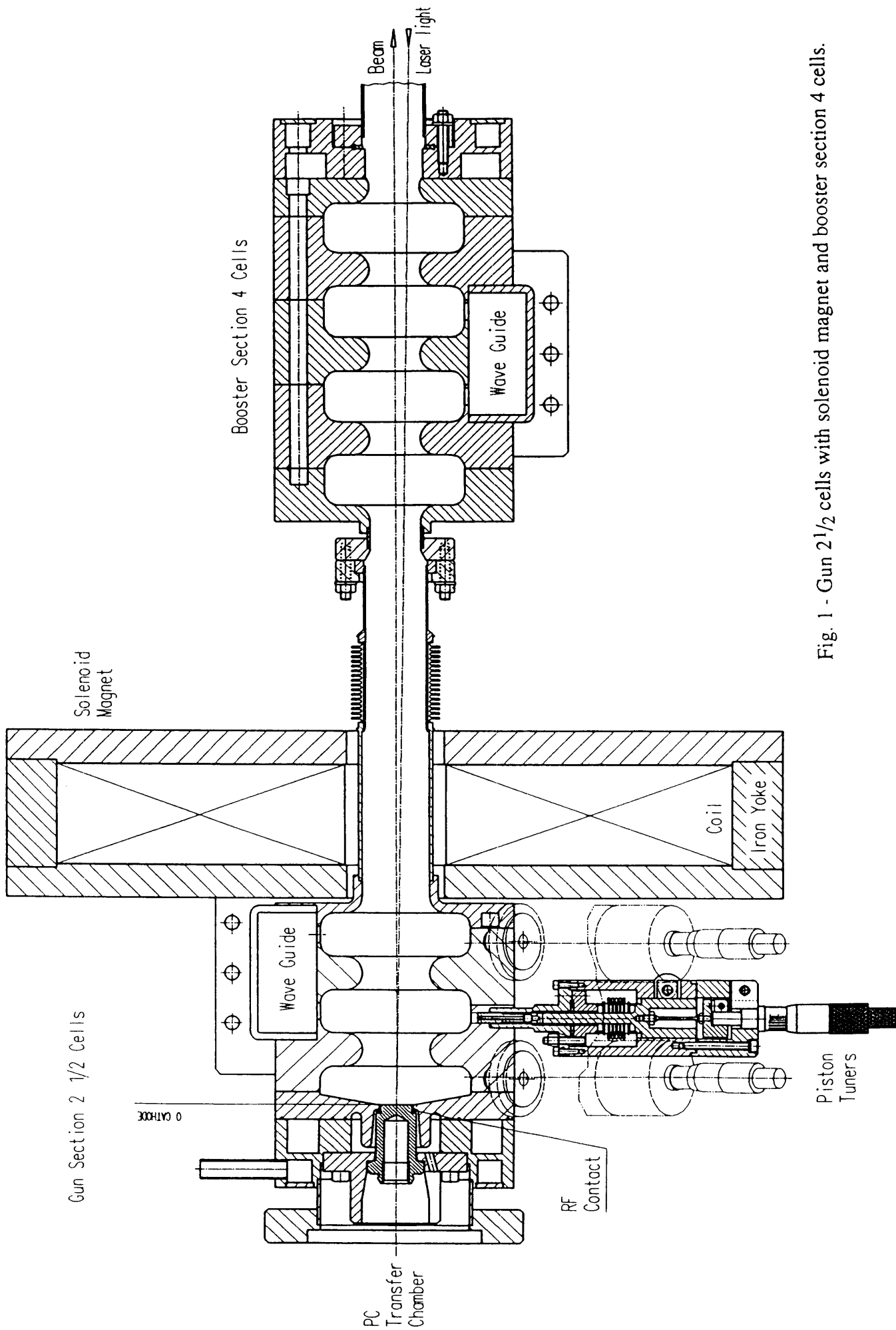


Fig. 1 - Gun 2 1/2 cells with solenoid magnet and booster section 4 cells.



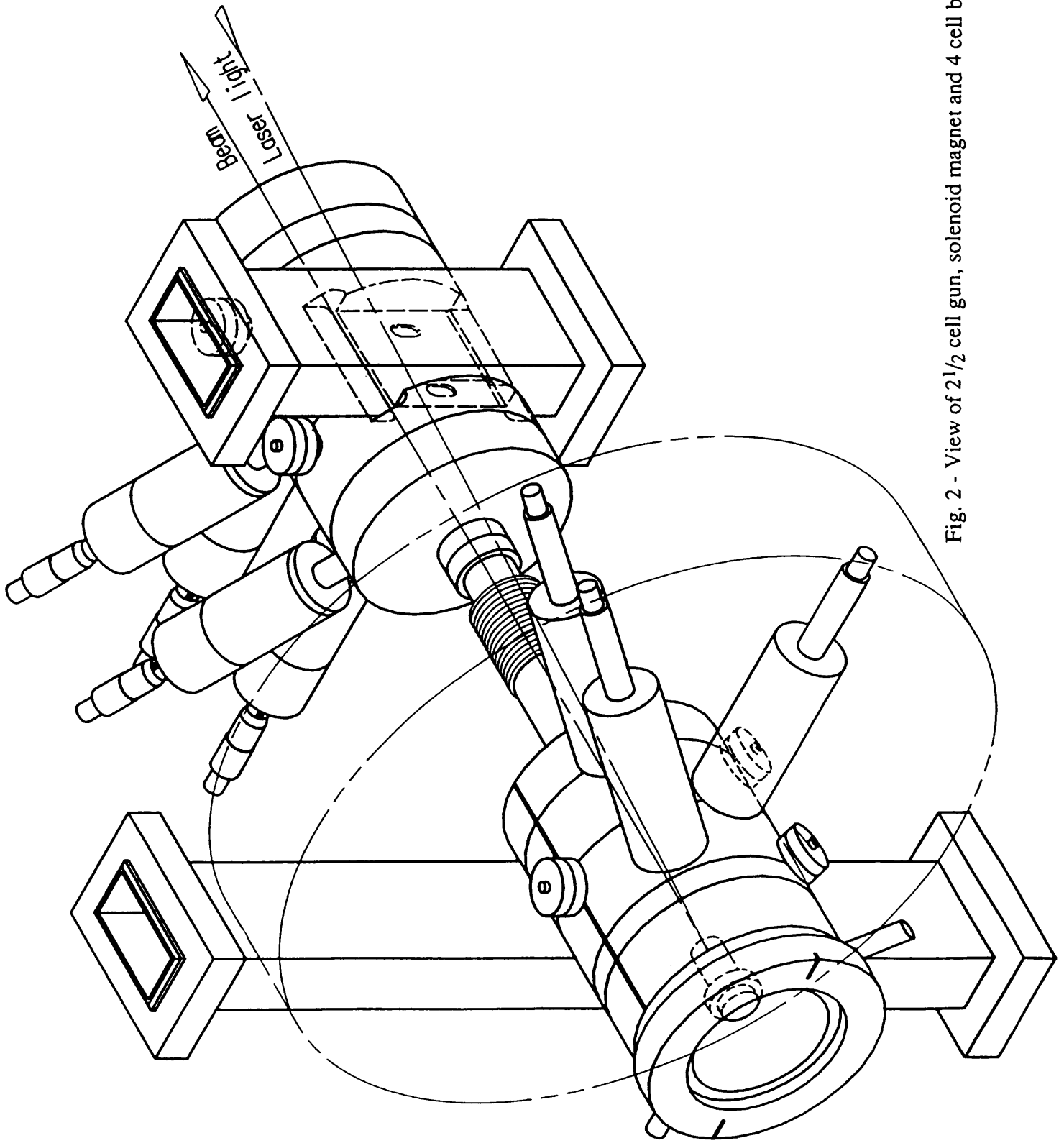


Fig. 2 - View of 2 1/2 cell gun, solenoid magnet and 4 cell booster section.

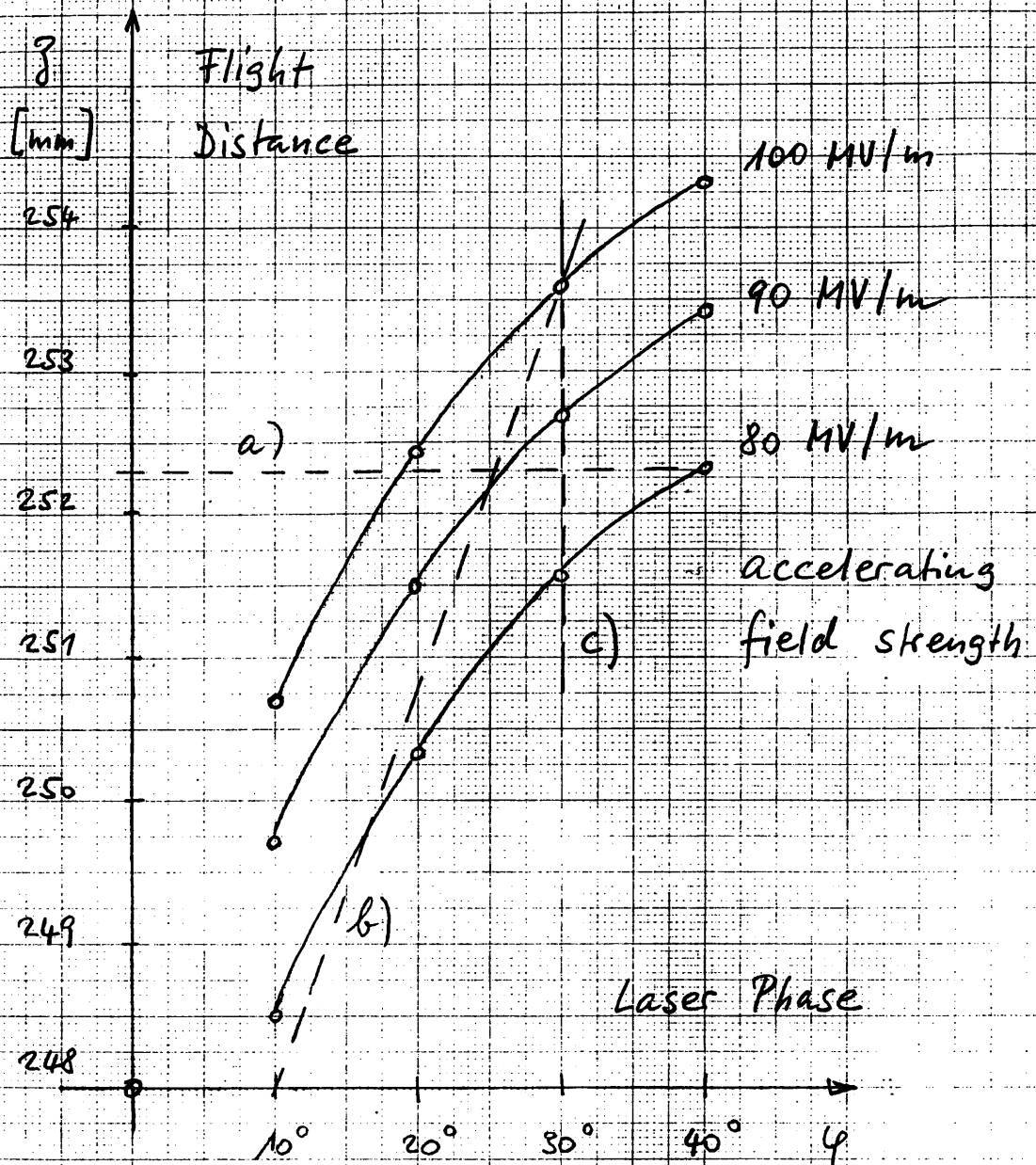


Fig. 3 Flight Path Table of Beam in Gun 4

for different field strength 100... 80 MV/m.

a) Gun phase shift  $\varphi = 19^\circ \dots 40^\circ$ ,  $\Delta z = 0.27 \text{ mm}$

b) Laser pulse train  $nL = n \times 99.92 \text{ mm}$ ,  $\Delta z = 0.25 \text{ mm}$

c) Laser pulse train  $nL = n \times 99.96 \text{ mm}$   
 + Gun phase shift  $\varphi = 30^\circ \dots 37^\circ$  }  $\Delta z = 0.12 \text{ mm}$

Residual Error of bunch spacing:  $\Delta z$

RB, 23.10.96